10-29-2003

Evaluation of Adsorption Effects on Measurements of Ammonia, Acetic Acid, and Methanol

Robert J. Yokelson
University of Montana - Missoula, bob.yokelson@umontana.edu

Ted J. Christian
University of Montana - Missoula

Isaac T. Bertschi
University of Montana - Missoula

Wei M. Hao
USDA Forest Service - Fires Sciences Laboratory

Recommended Citation

Yokelson, R. J., T. J. Christian, I. T. Bertschi, and W. M. Hao, Evaluation of adsorption effects on measurements of ammonia, acetic acid, and methanol, J. Geophys. Res., 108(D20), 4649, doi:10.1029/2003JD003549, 2003.

Evaluation of adsorption effects on measurements of ammonia, acetic acid, and methanol

R. J. Yokelson,[1] T. J. Christian,[1] I. T. Bertschi,[1,2] and W. M. Hao[3]

Received 28 February 2003; revised 20 June 2003; accepted 7 July 2003; published 29 October 2003.

[1] We examined how adsorption and desorption of gases from inlets and a cell could affect the accuracy of closed-cell FTIR measurements of carbon dioxide (CO_2), carbon monoxide (CO), methane (CH_4), nitric oxide (NO), nitrogen dioxide (NO_2), methanol (CH_3OH), acetic acid (CH_3COOH), and ammonia (NH_3). When standards were delivered to the cell through a stainless steel inlet, temporarily reduced transmission was observed for CH_3OH and NH_3. However, a halocarbon wax coated inlet (normally used on the system) had excellent transmission (comparable to room temperature Teflon) for both CH_3OH and NH_3, even at temperatures as low as 5°C. Thus the wax is valuable for coating sampling system components that cannot be fashioned from Teflon. The instrument had a delayed response (~10–40 s) for NH_3 only, which was attributed to passivation of the Pyrex multipass cell. To determine sampling artifacts that could arise from the complex sample matrix presented by smoke, the closed-cell FTIR system was intercompared with an open-path FTIR system (which is immune to sampling artifacts) in well-mixed smoke. A similar cell passivation delay for NH_3 was the only artifact found in this test. Overall, the results suggest that ~10 s is sufficient to detect >80% of an NH_3/CO ratio sampled by our fast-flow, closed-cell system. Longer sampling times or consecutive samples return better results. In field campaigns the closed-cell system sampling times were normally 10 to >100 s so NH_3 was probably underestimated by 5–15%. *INDEX TERMS:* 0315 Atmospheric Composition and Structure: Biosphere/atmosphere interactions; 0322 Atmospheric Composition and Structure: Constituent sources and sinks; 0345 Atmospheric Composition and Structure: Pollution—urban and regional (0305); 0365 Atmospheric Composition and Structure: Troposphere—composition and chemistry; 0394 Atmospheric Composition and Structure: Instruments and techniques; *KEYWORDS:* ammonia, acetic acid, methanol, halocarbon wax, surface passivation, trace gas sampling

Citation: Yokelson, R. J., T. J. Christian, I. T. Bertschi, and W. M. Hao, Evaluation of adsorption effects on measurements of ammonia, acetic acid, and methanol, *J. Geophys. Res.*, *108*(D20), 4649, doi:10.1029/2003JD003549, 2003.

1. Introduction

[2] Understanding Earth's atmospheric chemistry and climate requires widespread, accurate measurements of stable, reactive, and "sticky" trace gases [*Albritton et al.*, 1990; *Singh et al.*, 1995; *Roscoe and Clemitshaw*, 1997; *Mason et al.*, 2001]. Accuracy is compromised if trace gases react or stick to surfaces in sample inlets, storage containers, or instruments. Biomass burning is the second largest global trace gas source and open-path Fourier transform infrared (OP-FTIR) spectroscopy (immune to storage or surface-related artifacts) has shown that ~70–80% of the nonmethane organic compounds and many other species emitted by fires are reactive or sticky [*Crutzen and Andreae*, 1990; *Griffith et al.*, 1991; *Yokelson et al.*, 1996, 1997; *Worden et al.*, 1997; *Goode et al.*, 1999; *Bertschi et al.*, 2003a, 2003b; *Christian et al.*, 2003a, 2003b]. After the early OP-FTIR work, *Yokelson et al.* [1999] developed a lightweight, airborne FTIR (AFTIR) system for in situ measurements of the plumes from large fires, downwind chemistry, and other parts of the atmosphere. For reasons they discussed in detail, AFTIR measures the IR spectra of the contents of a gas cell inside an aircraft. In this paper, the AFTIR system was tested for sampling artifacts.

[3] The flow of air through AFTIR is driven by aircraft ram pressure so that no pumps or flowmeters are required and the associated weight, power, electronics, and maintenance are eliminated. A pair of pneumatic valves on the inlet and outlet of the cell allows continuous, real time measurements (valves open), or capture of "grab" samples by closing the valves and then scanning the sample repeatedly to improve the signal-to-noise ratio (SNR). The continuous, fast monitoring of the cell contents allows correction for any changes during storage in the cell [*Yokelson et al.*, 1999, 2003]. To minimize sampling losses, AFTIR employs fast flow; halocarbon wax coating [*Webster et al.*, 1994] on the metal, external inlet and cell-inlet valve; a Teflon sample line; and a Pyrex cell. However, potential losses during

[1]Department of Chemistry, University of Montana, Missoula, Montana, USA.
[2]Now at Interdisciplinary Arts and Sciences, University of Washington, Bothell, Washington, USA.
[3]Fire Sciences Laboratory, U.S. Department of Agriculture Forest Service, Missoula, Montana, USA.

0148-0227/03/2003JD003549

sample acquisition, on the inlet or due to cell passivation, required characterization. Prior to this work, a halocarbon wax coating was shown to have good passing efficiency for HCl [*Webster et al.*, 1994] and OH [*Bertram et al.*, 2001] and glass was known to be associated with passivation losses for HNO_3 and NH_3 [*van Hove et al.*, 1989; *Schiff et al.*, 1990; *Neuman et al.*, 1999; *Langmuir*, 1918]. This work measured the passing efficiency of our inlet coating and the passivation of our Pyrex cell for ammonia, acetic acid, methanol, and other compounds. The tests were run for sample matrices of varying complexity and at both room and reduced temperature ($\sim$5°C). Thus these results have general significance for analytical chemists. Since AFTIR is easily adapted for ground-based sampling by coupling a blower to the cell outlet, the characteristics of a system designed to exchange gases at ambient pressure rather than using pump/purge/fill cycles is of general interest.

2. Experimental Details

2.1. Overview of the Design and Use of the AFTIR System

[4] An overview of the design and in-flight use of the AFTIR system provides a context for the tests described in this paper. The AFTIR system obtains FTIR spectra of air flowing through, or detained within, a multipass cell inside an aircraft [*Yokelson et al.*, 1999, 2003; *Goode et al.*, 2000]. Outside air is forced by ram pressure into a 22 mm i.d., forward-facing inlet that is 32 cm long and opens 28 cm from the outer skin of the aircraft cabin roof. The air (now inside the cabin) then flows through 10 m of 25 mm i.d. flexible, Teflon bellows; a 15 l Pyrex cell; and $\sim$5 m of 25 mm i.d. tubing to a rear-facing outlet. Fast-acting valves (19 mm i.d.) on the inlet and outlet of the cell are used to temporarily trap the cell contents for signal averaging at desired times. The valves are built in-house and driven by a small compressed air source. Each is composed of a coated metal butterfly valve (Milwaukee Valve BB2-100), a pneumatic actuator (Bettis RPC-250), and a solenoid (Skinner Valve type 73417) controlled by a custom circuit. In airborne deployments the volume flow rate through the system was $\sim$100–240 liters per minute (Lpm). The residence time in the exterior inlet is $\sim$30–70 ms. The residence time in the part of the inlet inside the aircraft (normally warmer than ambient air) is $\sim$1–2 s. Sample air had reached cabin temperature (12–33°C) upon entering the cell. These flows and residence times supersede those reported by *Yokelson et al.* [2003] (see section 3.1).

[5] Infrared spectra of the cell contents are acquired every 0.83 s throughout most of each flight and the flow-control valves are normally open, which flushes the cell with ambient air. The object when sampling plumes is to accurately measure the ratios between the excess amounts of the gases in the plumes. To temporarily trap smoke plume "grab" samples we fly into a plume and then close the valves 10 to >100 s later when the cell is well flushed with smoke. The valves remain closed for 1–3 min while several hundred spectra of the sample are acquired. The cell is flushed for >2 min before background grab samples are trapped at the same altitude just outside the plume (before or after samples) and processed in the same way.

[6] The IR optical system used to quantify the cell contents is described elsewhere [*Yokelson et al.*, 1999]. Briefly, it features a 0.5 cm^{-1} resolution FTIR (MIDAC model 2500) with the IR beam directed through tripled White cell optics [*White*, 1942] enclosed in the Pyrex cell and onto an LN_2-cooled MCT (mercury-cadmium-telluride) detector. Temperature and pressure are measured in the cell and the mixing ratios for the trace gases are retrieved from the IR spectra with custom software [*Yokelson et al.*, 1996, 1997; *Yokelson and Bertschi*, 2002].

2.2. Overview of the Test Configurations

2.2.1. General Experimental Considerations

[7] In phase 1, AFTIR (coupled to various inlet materials) measured standards mixed in a carrier gas flow at both room and reduced temperature. In phase 2, a range of possible effects due to the other components of smoke (water, particles, etc...) was investigated by codeploying AFTIR with our open-path FTIR in well-mixed smoke. An important experimental constraint is that passivation of surfaces is faster at higher analyte concentrations [*Neuman et al.*, 1999]. Our tests were designed to determine if passivation of the inlet or cell affects our results at the levels of trace gases we encounter in the field in smoke plumes (20–500 ppb). Thus, rather than run the tests at high mixing ratios where SNR is optimized, we used levels <300 ppb where we obtained slower passivation, bigger fractional losses (of a less abundant standard), and more relevant results. The AFTIR detection limit for most compounds is 5–20 ppb for $\sim$100 scans and $\sim$20–100 ppb for single scans. Thus the uncertainty in much of the data is $\sim\pm$10–30% (based on SNR).

2.2.2. Configuration of Tests With Standard Mixtures

[8] This phase of the testing followed the work of *Neuman et al.* [1999] in which an HNO_3 standard was delivered through tubing made from a variety of materials used in instrument construction to a fast HNO_3 detector and delays (or failure) in reaching the delivered concentration were attributed to passivation losses on the test material. *Neuman et al.* [1999] found that Teflon was the best material, but HNO_3 did stick to it reversibly below $\sim$10°C. Our procedure was slightly different. Since the AFTIR cell may require >30 s to completely exchange, we compared the temporal profile for reaching a delivered amount of a test gas to the temporal profile for reaching a delivered amount of a simultaneously introduced "nonsticky" tracer (CO). We also used faster flows to simulate our field sampling flow rates.

[9] Figure 1 is a simplified representation of the plumbing for the phase 1 tests. The entire system for gas delivery to AFTIR was assembled using Teflon tubing, valves, and fittings, except for the flow controller, flowmeters, and some needle valves, which had stainless steel, nickel, or Viton® parts. These devices were, however, only employed upstream of the introduction of any problematic gases. The primary carrier gas flow to AFTIR was controlled with a 100-sLpm (standard liter per minute) mass flow controller (MKS 1500) accurate to ±1.0% of full scale. Carrier gas (CG) flow for these experiments ranged from 25 to 100 sLpm. Since cell temperature was 22–25°C (standard is 0°C) and cell pressure was $\sim$0.9 atm, the range in volume flow rates was $\sim$30–121 Lpm. The upper end of this range overlaps the flow rates in airborne deployments of the AFTIR system. The ultra high purity (UHP) nitrogen that we purchased for use as

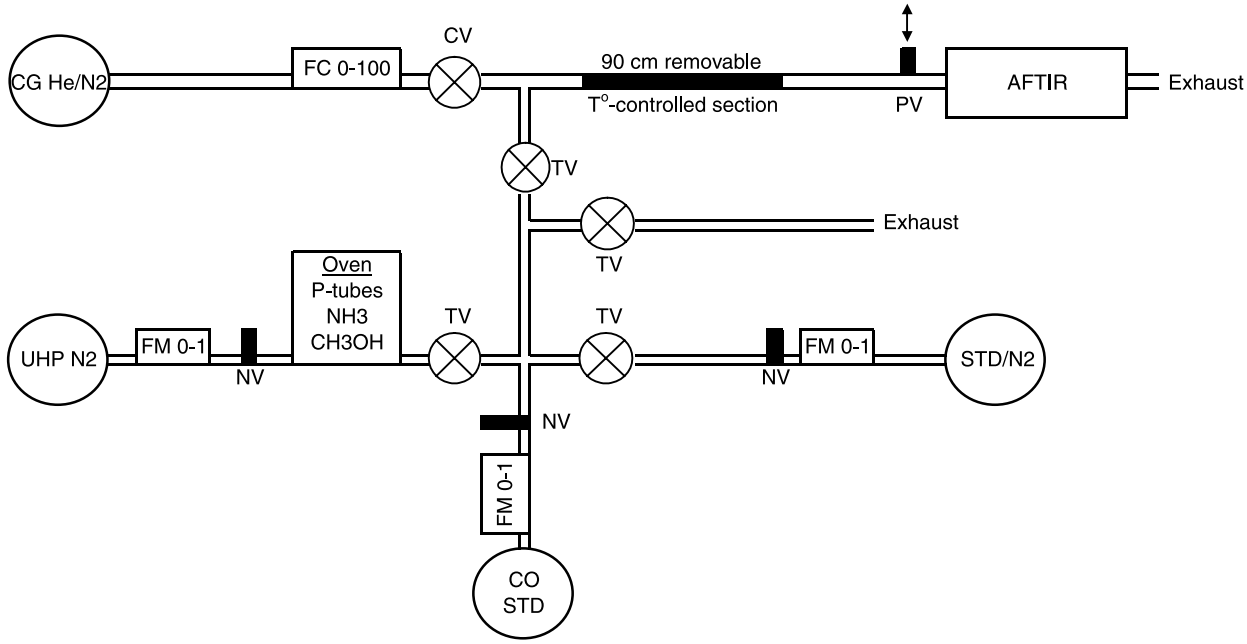

Figure 1. A simplified schematic of the system built to deliver standards to AFTIR. CG, carrier gas; FC, flow controller (mass flow range in standard liters per minute); CV, control valve; PV, pneumatic valve (halocarbon-wax coated); TV, Teflon valve; FM, flowmeter; NV, needle valve; STD, standard. The regulator and shutoff on each gas tank is not shown.

a CG contained 670 ppbv CO as determined by three separate analyses using gas chromatography and FTIR. The helium we obtained was essentially "CO-free." Since CO was used as a stable tracer in the experiments and because of the spectral noise (at some frequencies) that accompanies a fast flow of N_2 through AFTIR, the majority of tests were run using He CG to allow continuous monitoring at all frequencies. Some stopped-flow experiments or higher-noise runs with N_2 CG were done to spot check for effects of the CG.

[10] Flow from a 100 ppmv CO standard in N_2 (EPA protocol, ±1%) was routed through a 1.0 sLpm mass flowmeter and a needle valve to a Teflon valve that allowed introduction at desired times into the CG stream. The mixing ratio of additional, "non-CG" CO delivered to AFTIR (typically 200–500 ppbv) was simply: (CO-line flow/total flow) * (mixing ratio of standard). CO_2, CH_4, CH_3OH, NO, and NO_2 standards in cylinders (20,000, 9.65 (NIST), 106, 104, and 99 ppmv, all ± ≤2%) were also routed through a flowmeter and needle valve and then premixed with the CO standard before introduction to the CG stream. Delivery mixing ratios (~100–300 ppbv) were calculated using the method above. Permeation tubes (20 cm length; VICI Metronics, Inc.) that emitted NH_3 (7730 ± 2% ng/min at 35°C) or CH_3OH (22,560 ± 2% ng/min at 80°C) were held at constant temperature in a calibrated oven (Dynacalibrator model 190) and the output was entrained into a small, measured flow of UHP N_2. The oven output was premixed with the CO standard before introduction to the CG stream. The mixing ratios delivered to AFTIR (for oven output) were calculated from the constant mass-loss rate for the tube and the total flow. They ranged from 101–202 ppbv for NH_3 and 199–273 ppbv for CH_3OH.

[11] A 90 cm section of the 2 m Teflon tubing connecting the standards with AFTIR was removable, allowing tests of two separate sections of 1.6 × 90 cm, 316 stainless steel tubing. Both tubes were cleaned with mild laboratory soap and then thoroughly rinsed and dried. One section was used uncoated and the other was used after coating with the same halocarbon wax (1500 Grade, Halocarbon Products Corp., River Edge, NJ) and application technique used in AFTIR. We have applied halocarbon wax by melting it onto surfaces, but caution must be taken not to exceed the liquid range and to ensure a continuous coating. When the wax is dissolved in methylene chloride, using a magnetic stirrer (faster than ultrasound), it is easier to apply a continuous layer to the inside of tubes. The methylene chloride is removed by drying at 60–100°C for several days followed by mild vacuum. Halocarbon (and paraffin) wax coatings were shown to be smooth and nonporous by *Bertram et al.* [2001], and difficult to wet [*Benner et al.*, 1992; *Bertram et al.*, 2001]. The metal tubes were ~3 times longer and 30% narrower than the combination of the AFTIR external metal inlet and inlet valve. Thus any problems observed with the coating would reflect ~3 times the exposure to a coated surface as occurs in actual use of the AFTIR system (for a given flow rate). The temperature of the stainless steel inlet sections was controlled by winding them with 0.635 cm o.d. copper tubing connected to a refrigerated, recirculating bath (Forma Scientific model 2095) and then insulating the assembly with 1.27 cm-thick foam. The inlet sections were tested at 4.8°C, 9°C, and at room temperature (22–25°C). Gas exiting a cooled inlet returned to room temperature before it entered the AFTIR cell.

[12] Reynolds number calculations indicate laminar flow (R_e < 2000) within the AFTIR cell for all flow rates and carrier gases used. The nature of the flow within the inlet

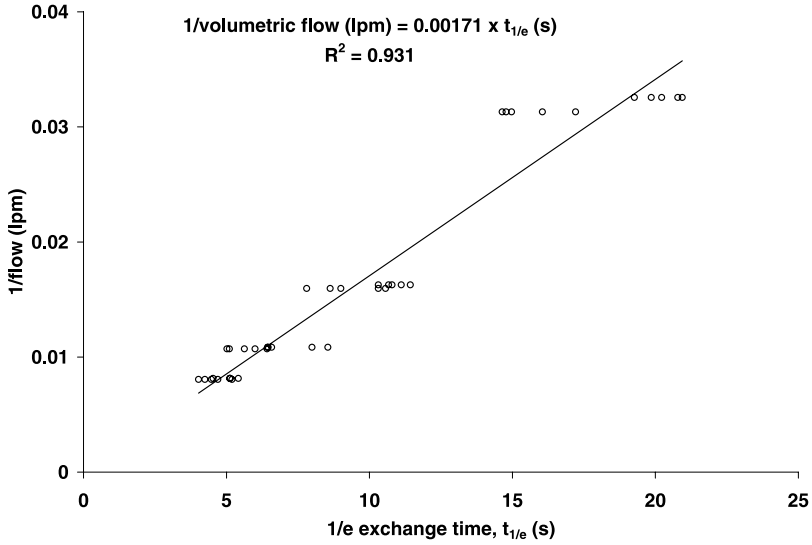

Figure 2. The reciprocal of the volume flow rate versus the CO 1/*e* exchange time, $\tau_{1/e}$, for the AFTIR cell.

depended on the CG. When He was the CG, R_e never exceeded 1800, indicating laminar flow. However, for N_2, R_e exceeded 2800 in all cases.

2.2.3. Configuration for Codeployment of Open-Path and Closed-Cell FTIR in Well-Mixed Smoke

[13] The above tests determine the effects of various surfaces and temperatures on individual compounds in a low-humidity carrier gas flow. Under field conditions, artifacts could arise due to the presence of many other components in the sample matrix. For instance, one can speculate that the high levels of water and CO_2 in combustion emissions could lead to the formation of carbonic acid on inlet/instrument surfaces and change their properties. To individually investigate all the effects possible due to the interactions between surfaces and all the components of smoke is beyond the scope of any experiment. We adopted a novel approach to check for AFTIR sampling artifacts in "real" smoke that entailed comparing AFTIR to our open-path FTIR in well-mixed smoke. The OP-FTIR system was deployed so that it's 1.6 m basepath, open White cell spanned the smoke plume rising through a stack above a gently smoldering fire in the USDA Forest Service, Fire Sciences Laboratory combustion facility [*Yokelson et al.*, 1997; *Christian et al.*, 2003a, 2003b]. The OP-FTIR continuously quantified the slowly changing trace gases. The OP-FTIR has an identical spectrometer, but no inlet or enclosed sample cell so it is not subject to sampling- or storage-related artifacts [*Yokelson et al.*, 1997; *Goode et al.*, 1999; *Bertschi et al.*, 2003a, 2003b; *Christian et al.*, 2003a, 2003b]. This provides a benchmark against which any sampling artifacts in AFTIR can be quantified. An inexpensive, oil-free blower on the outlet of the AFTIR generated a flow of 206–265 Lpm (overlapping the high end of our airborne flow rates). For this test, we used the AFTIR Teflon sample line as an inlet, which was periodically inserted just above the center of the OP-FTIR path. Using the AFTIR cell inlet/outlet valves we sampled the emissions at 17 known times with respect to the OP-FTIR data using different "cell exchange" or "sample-acquisition times" ranging from 4.1 to 64.2 s. AFTIR was flushed with clean air between smoke samples.

[14] The requirement that the smoke sampled by the open-path and point-sampling techniques is well mixed is critical to the interpretation of these results. Three separate tests confirmed this for the smoke at the sampling platform of the combustion facility. (1) The temperature profile across the stack is "flat" even as the temperature changes during a burn. (2) The agreement between OP-FTIR and point-sampling into canisters for 6 gases was within 1σ for 8 of 10 comparisons and within 2σ for the remaining two [*Goode et al.*, 1999]. (3) The ratio between the OP-FTIR and a point sampling PTR-MS was independent of the distance of the point-sampling location from the stack wall: even for sticky compounds such as acetic acid [*Christian et al.*, 2003a].

3. Results and Discussion

3.1. Results of the Tests in Standard Mixtures

[15] First, we reexamined the flow rate through AFTIR obtained during flight. We had previously estimated this using the approximate 1/*e* exchange time ($\tau_{1/e}$) for CO when the smoke-filled cell was opened instantaneously and flushed with clean air, assuming plug flow in the cell. With the apparatus shown in Figure 1, we measured $\tau_{1/e}$ and τ_{95} for CO versus measured flow rates. At higher flows the exchange was approximately exponential in that τ_{95} was ~3 times $\tau_{1/e}$, but at lower flows the exchange was more sigmoidal. A logistic curve was used to fit all exchanges and solved for $\tau_{1/e}$ and τ_{95}. In Figure 2, the reciprocal of volume flow rates from 31 to 124 Lpm (25 to 101 sLpm) is plotted linearly against $\tau_{1/e}$ (which was independent of CG). In AFTIR deployments on a King Air B-90 [*Yokelson et al.*, 1999; *Goode et al.*, 2000], with a 19 mm i.d. inlet, $\tau_{1/e}$ for CO was ~4–5 s indicating flows of 117–146 Lpm (95–119 sLpm). On the University of Washington Convair 580 [*Yokelson et al.*, 2003], with the inlet described in section 2.1, $\tau_{1/e}$ was ~2.39–3.34 s (at airspeeds from 80–110 m/s)

indicating flows of 175–244 Lpm (130–150 sLpm). The results verify that our tests were conducted at relevant flow rates.

3.1.1. Results With Teflon Inlet

[16] Tests were conducted with all-Teflon plumbing so that the effects of uncoated/coated steel as an inlet could be isolated by comparison. In these tests, a stable, controlled flow of carrier gas was established through the cell while a mixture of the CO-standard tracer and the test gas flowed stably to a dump. At a selected time, valves were switched so that the premixed flow of CO and test gas instantaneously joined the CG flow into the cell. Any lag in the test gas rise in the cell in comparison to the rise of CO was taken as evidence of passivation losses.

[17] The rise profiles for CO_2, CH_4, NO, NO_2, CH_3OH (cylinder or oven), and NH_3 standards were compared (in turn) to that of the premixed, codelivered CO standard with a variety of CGs and flow rates. For all the test gases except NH_3, the rise profiles were not significantly different from that of CO (and independent of CG) indicating that no passivation losses were occurring in the system for CO_2, CH_4, NO, NO_2, and CH_3OH (Figures 3a and 3b). In contrast, at the same flow shown in Figures 3a–3b (58 sLpm), $\tau_{1/e}$ and τ_{95} for NH_3 were 11.45 and 39.1 s compared to $\tau_{1/e}$ and τ_{95} for CO of 7.12 and 21.8 s. Since $\tau_{1/e}$ is measured more accurately than τ_{95}, we define $\tau_{1/e}(NH_3) - \tau_{1/e}(CO)$ as the NH_3 passivation lag time (or "lag time") as one measure of adsorption effects. The NH_3 lag time in Figure 3c is 4.33 s. In addition, there was a "symmetrical delay" in the decay of NH_3 once the standard mixture was shut off ($\tau_{1/e}$ = 11.9 s, Figure 3d). Figure 3d suggests that if consecutive samples are obtained within ~100 s, the passivation lag is noticeably smaller for the second sample, but also that the cell should be flushed for 2–3 min before acquiring a background sample. When the Teflon inlet was shortened from 200 to <30 cm, the NH_3 lag time did not change (4.58 s), suggesting that the passivation losses occur mainly on the AFTIR Pyrex cell. These effects were reproducible: even for runs that were done before and after cleaning the cell on a field campaign in Africa. The effects are also consistent with the fact that NH_3 was the only compound found to exhibit fast losses when detained in the Pyrex cell [*Yokelson et al.*, 1999, 2003]. For example, in a separate experiment, the NH_3 mixing ratio was brought to ~100 ppbv and the cell inlet and outlet valves were closed: subsequently the mixing ratio dropped by 10% in 40 s. These storage losses are already routinely corrected.

[18] Fast system flow rates have the advantage of reducing the percentage of analyte (including those not tested here) that contacts the system walls. In addition, for a given mixing ratio, system passivation could be faster at high flow since the cell-exchange time is reduced and the mass flow rate is increased. We did not directly test this hypothesis in this work because our gas system delivered a single, constant NH_3 mass-flow rate. Thus increasing the flow simultaneously reduced the delivered mixing ratio (which would tend to slow passivation). However, indirect evidence suggests that faster flow would speed passivation at a fixed mixing ratio. For instance, in back-to-back runs at 58 and 101 sLpm the measured/actual NH_3/CO ratio reaches unity faster at the higher flow rate despite the lower concentration, but the data are noisy. A more detailed analysis that incorporates 3 runs at 58 sLpm, 1 run at 79.5 sLpm, and 2 runs at 101 sLpm suggests that all the passivation rates are statistically similar despite the fact that high flow was associated with reduced concentrations, which would have tended to slow passivation (Figure 4). The indirect implication is that the slowing effects of reduced concentration were compensated by a tendency for faster flow to hasten passivation. We conclude that, for a fixed concentration, higher flow would speed passivation.

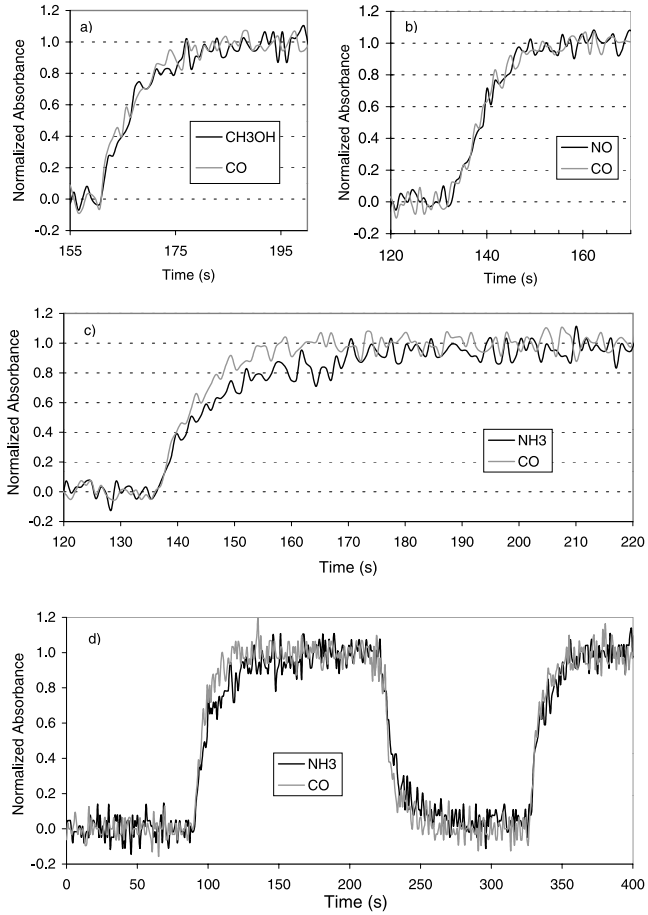

Figure 3. NH_3 compared to gases that track CO at 58 sLpm total flow (see text).

[19] Despite the passivation losses, the NH_3 rise time was not measurably dependent on CG, which would affect diffusion rates. Because of the higher noise with flowing N_2 CG, we performed four "stopped flow" experiments in N_2 to verify the lag time independence of CG for NH_3 (Figure 5). With a CG flow of 50 sLpm N_2, we waited 2 min once and 10 s 3 times before closing the AFTIR valves to enable a high SNR NH_3 analysis in N_2. When waiting 2 min to close the valves the measured NH_3/CO was the delivered ratio. When waiting 10 s, the measured NH_3/CO was 75.7 ± 2.1% of the delivered NH_3/CO, which is not significantly different from the ratio measured at 10 ± 3 s in He at 58 sLpm (Figure 4). We note that these NH_3 passivation losses are at flow rates below our field flow rates of >100 sLpm so the losses should be smaller in the field, since passivation is evidently faster at increased flow. In summary, these tests show that: (1) AFTIR

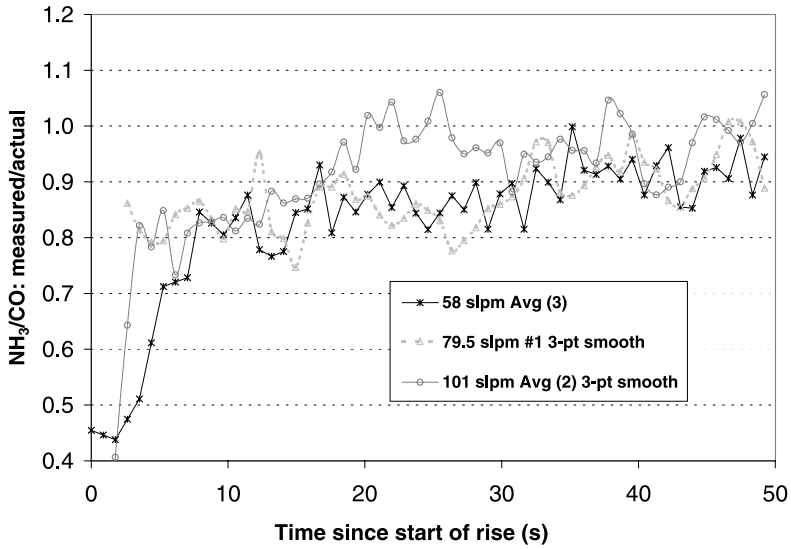

Figure 4. Cell passivation rates for NH_3 at different total flow rates (see text).

performed well for many compounds. (2) Even with no significant inlet losses, the Pyrex cell leads to small, temporary passivation losses for NH_3. (3) Longer sample acquisition times or consecutive samples (as long as the interval between samples is sufficient to avoid cross-contamination) return more quantitative results. (4) Teflon coating the Pyrex cell may decrease the cell passivation time.

3.1.2. Results With Coated or Uncoated Stainless Steel Inlets

[20] When 90 cm of the Teflon inlet was replaced by room temperature stainless steel, the NH_3 lag time (at 58 sLpm) increased from 4.33 to 6.95 s (Figures 3c and 6a). However, when the stainless steel inlet section was coated with halocarbon wax, the NH_3 lag time was the same (3.85 s) as with the Teflon inlet (Figure 6b), even at ~5°C where the lag on uncoated steel was larger than at room temperature. There was also a significant passivation lag time for methanol on cold uncoated steel (2.43 s), but this lag was very small on cold, coated steel. Our methanol results are analogous to formaldehyde (HCHO) results reported by *Wert et al.* [2002]. They observed HCHO passivation delays (at 1 sLpm) on uncoated steel inlets that were longer at low temperature, but good performance on silica-coated steel inlets even at low temperature. In summary, (1) even with an uncoated steel inlet AFTIR worked well for many compounds. (2) Uncoated steel always caused additional losses for NH_3 and cold, uncoated steel caused losses for CH_3OH. (3) Using the halocarbon wax to coat the steel gave it performance similar to Teflon down to 5°C: thus, the coating is recommended for sampling these compounds.

3.2. Results of Codeploying Open-Path and Closed-Cell FTIR in Well-Mixed Smoke

[21] For this test, the AFTIR and OP-FTIR system were codeployed in slowly changing, well-mixed smoke in the

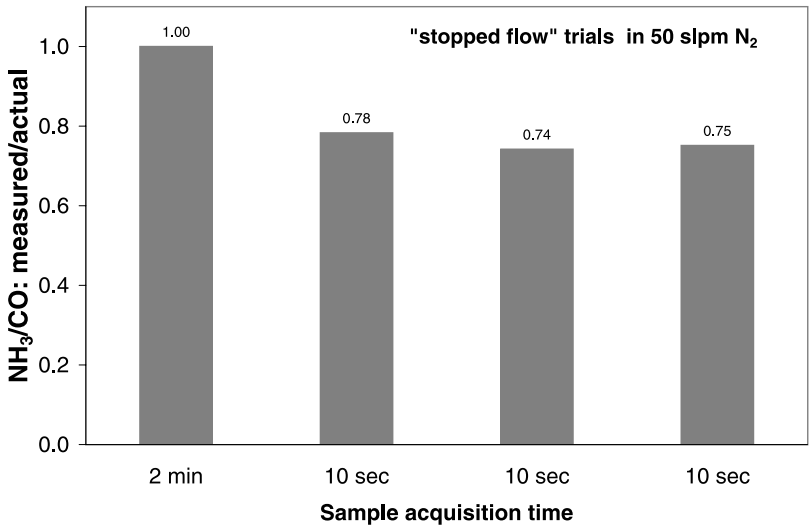

Figure 5. The NH_3 passivation rate for the AFTIR cell is similar in N_2 and He (Figure 4, see text).

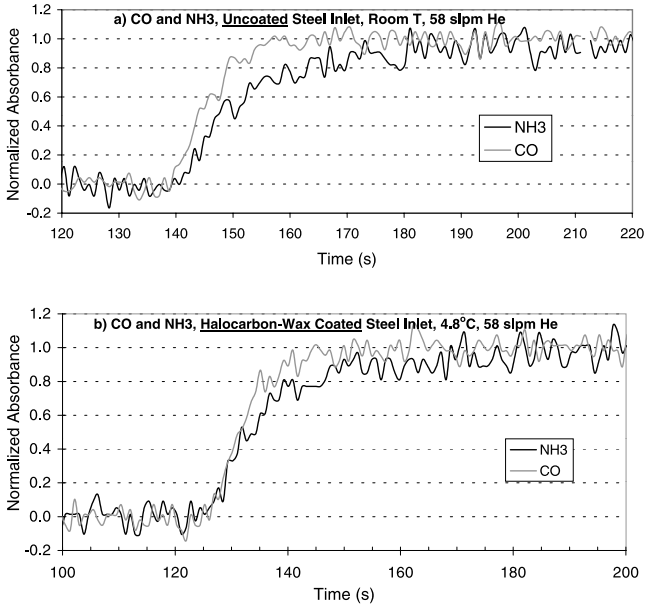

Figure 6. The passivation lag for NH_3 is longer with (a) an uncoated steel inlet than with a Teflon inlet (Figure 3c). However, the passivation lag for NH_3 with (b) a halocarbon-wax, coated steel inlet is the same as with a Teflon inlet even at low temperature.

combustion facility stack as described earlier. Because the background levels of CO, CO_2, and CH_4 were substantial and somewhat variable, we used another major smoke component, ethene (C_2H_4), as the nonsticky tracer in these tests [*Goode et al.*, 1999]. For each AFTIR sample, the ratio of NH_3, CH_3COOH, and CH_3OH to C_2H_4 was determined from the AFTIR spectrum and compared to the analogous ratio measured independently at the sampling time by OP-FTIR. An AFTIR ratio substantially below that of OP-FTIR indicates sample losses associated with the AFTIR cell. The results of this test are shown in Figure 7a. As expected, when using very short sample acquisition times, AFTIR underestimated the NH_3/C_2H_4 ratio. However, even at the shortest sample acquisition time, the AFTIR ratios for CH_3OH/C_2H_4 and CH_3COOH/C_2H_4 were not significantly lower than the OP-FTIR ratios. At sample acquisition times of 10 ± 2 s the AFTIR NH_3/C_2H_4 ratios range from 77–97% of the "delivered value;" slightly above the 10 s average in the simple mixture tests (Figures 4 and 5), but the difference is not statistically significant.

[22] Since the passivation rate should depend on the mixing ratio, we also plot the AFTIR/OP-FTIR ratios as a function of the product of sample acquisition time and "actual" ppm NH_3 (SAT * NH_3) in Figure 7b. (The representation of these results in Figure 7b may have some application to sampling NH_3 at lower levels.) Again, the agreement with the simple mixture tests is good. For the data in Figure 5, the product SAT * NH_3 was 2.0 s ppmv and the average ratio of measured to delivered NH_3/CO was 75.7 ± 2%. In Figure 7b, the five runs with an SAT * NH_3 of 2 ± 1 s ppmv have a similar average value of 76.8 ± 6%. This result (although from two different flow rates) indicates that shortfalls in real smoke, which were detected only for NH_3, are mainly due to the interaction between Pyrex and NH_3. No new sampling artifacts could be assigned to the more complex sample matrix.

3.3. Implications of the AFTIR Test Results

[23] The only sampling artifact affecting the AFTIR system, as normally used with a halocarbon wax-coated inlet, was a brief (10–40 s) passivation delay for NH_3, which was attributed to the Pyrex cell. Cell passivation rates were independent of carrier gas, but should be hastened by higher concentrations or flow rates. Teflon-coating the Pyrex cell may reduce or eliminate passivation lags. However, the good performance of Teflon (or coated steel) for NH_3 may be specifically for fresh surfaces since *Lee et al.* [1991] detected H_2O_2 losses on degraded Teflon. It is worth noting that an all-Pyrex sampling/storage system is used in a new NH_3 instrument [*Owens et al.*, 1999] and that the EPA requires the use of glass for sampling NH_3 [*Environmental*

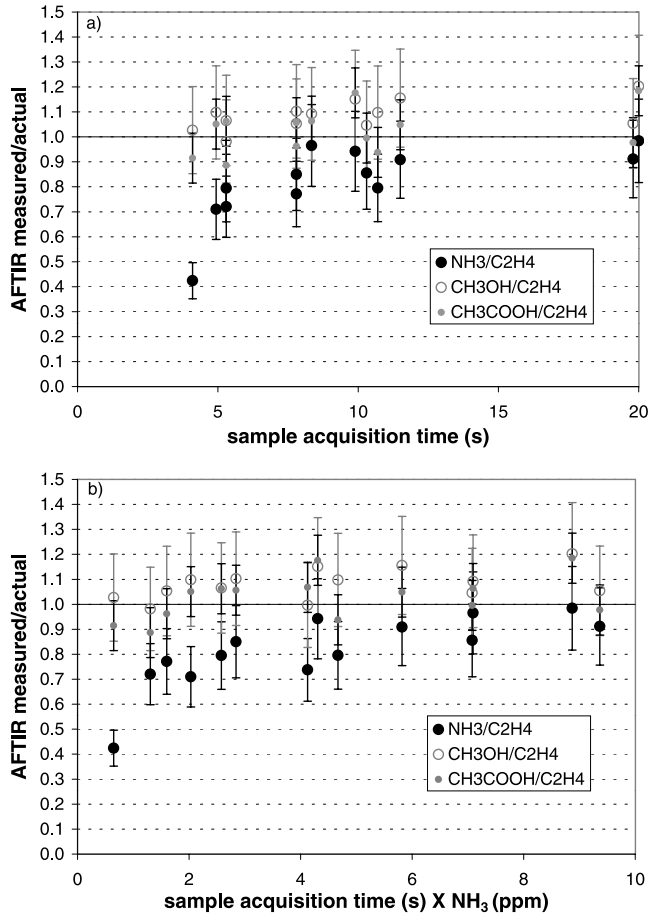

Figure 7. The ratio of three different trace gases to C_2H_4 (as measured by AFTIR) compared to the ratio determined by OP-FTIR (which is immune to sampling artifacts) in well-mixed smoke. (a) The independent axis is the length of time that each smoke sample was drawn into the AFTIR Pyrex cell. Four samples at longer sample acquisition times are not shown to highlight details at the shorter times. (b) The independent axis is the sample acquisition time multiplied by the sample-specific, absolute NH_3 mixing ratio measured by OP-FTIR. These values ranged from 148 to 802 ppb.

Protection Agency, 1982]. Our results indicate that sampling NH_3 with glass requires great caution.

[24] Since, depending on flow rate, AFTIR required ~40–60 s for complete exchange of nonsticky gases and up to 2 min to complete adsorption or desorption of NH_3, one could measure absolute mixing ratios (at the levels tested) with a similar closed cell system if sample concentrations change slowly (i.e., a few percent per minute). In quickly changing air, or when sampling plumes of limited extent from a rapidly moving platform, there are additional considerations. In these cases, the cell mixing ratios may not be identical to the rapidly changing absolute ambient values. However, in plume sampling, the absolute levels strongly reflect the instantaneous amount of plume dilution and the more important measurement is usually the ratio between compounds as explained by *Yokelson et al.* [1999]. With plume sample acquisition times of ~10 s the proper ratios between compounds should be returned for most compounds and the error for NH_3 was ~15% (Figure 7a). Longer sample times or sufficiently spaced, consecutive samples are better. We randomly selected 7 smoke samples from our recent airborne campaign in Africa and measured the sample acquisition times. They ranged from 16 to >100 s. We also frequently obtained consecutive samples. Thus the error in the NH_3 mixing ratios in previous studies was probably 5–15%, but difficult to quantify; especially since instrument performance could change over the years [*Yokelson et al.*, 1999, 2003; *Goode et al.*, 2000].

[25] We did not conduct any tests at relative humidities (RH) >50%. However, at longer residence times (>30 s), losses of NH_3 have been observed in water films that formed on the surfaces of leaves or glass at RH $\geq$ 60% [*van Hove et al.*, 1989]. All our field measurements of fires were at RH < 50% except in Mozambique (RH 55–60%) and smoky clouds (RH 100%). Relevant to the influence of RH on inlet and cell performance we note: (1) The compression/heating of the air ahead of the forward-facing AFTIR inlet has the net effect of reducing the RH of air entering the inlet by ~40% [*Webster et al.*, 1994]. Thus cloud samples have RH of ~60% in the "exterior" inlet. The RH in the rest of the inlet and cell system is lower. (2) The RH required to form significant water films depends on the surface. At 68% RH, water films that caused loss of SO_2 formed on glass, but not on wax, even after 12 hours. At 90% RH, water films caused losses on both surfaces [*Benner et al.*, 1992]. Adsorption of HNO_3 on an unheated Teflon inlet dropped below 10% within a few seconds at RH < 60%, but the same reduction in adsorption required several minutes at RH near 100% [*Neuman et al.*, 1999]. (3) Significant losses in water films require sufficient interaction. The NH_3 losses on water-coated glass and leaves were not detected above flow rates of 5–6 sLpm (residence time of 30 s) [*Sauren et al.*, 1989]. *Wert et al.* [2002] detected no losses for an uncoated, unheated, steel inlet at 12 sLpm and RH of 85% for HCHO. (Both HCHO and HNO_3 have a higher solubility than NH_3.) In summary, AFTIR features RH reduction ahead of the inlet, fast flow, and a hydrophobic halocarbon wax coating on the inlet. Therefore AFTIR is probably affected minimally by high RH. However, for instruments with longer residence times in unheated plumbing, a halocarbon wax coating (or Teflon) would probably not prevent sampling artifacts at high RH.

[26] Finally, the intercomparison between OP-FTIR and AFTIR in well-mixed smoke is a generally useful approach for testing many point-sampling instruments. We recently intercompared our OP-FTIR with a proton transfer mass spectrometer [*Holzinger et al.*, 1999] and stainless steel canisters [*Christian et al.*, 2003a].

4. Conclusions

[27] NH_3 and CH_3OH were temporarily adsorbed on stainless steel inlets, but halocarbon wax coated steel had passing efficiency similar to room temperature Teflon for both compounds despite temperatures as low as 5°C or complex sample matrices. Thus the wax has been used to impart excellent passing efficiency to steel for both basic (NH_3, this work) and acidic (HCl [*Webster et al.*, 1994]) compounds. All detected effects in these tests were due to interactions between NH_3 and Pyrex or uncoated steel; or interaction between CH_3OH and cold, uncoated steel. No additional effects due to the many other components of smoke were observed. For normal use of the airborne FTIR (AFTIR) system tested, the only sampling artifact was a 10–40 s delayed response for NH_3, which was attributed to passivation of the Pyrex cell. Mostly due to the limited width of some of the plumes sampled, previous NH_3 measurements by AFTIR were probably 5–15% too low.

[28] **Acknowledgments.** This research was supported by funds provided by the National Science Foundation under grant ATM-9900494, the Interagency Joint Fire Science Program, and the Rocky Mountain Research Station, Forest Service, U.S. Department of Agriculture (INT-97082-RJVA and RMRS-99508-RJVA). We thank Carl Howard, Greg Huey, Andy Neuman, and the anonymous reviewers for guidance and comments on this work.

References

Albritton, D. L., F. C. Fehsenfeld, and A. F. Tuck, Instrumental requirements for global atmospheric chemistry, *Science*, *250*, 75–81, 1990.

Benner, W. H., B. Ogorevc, and T. Novakov, Oxidation of SO_2 in thin water films containing NH_3, *Atmos. Environ.*, *26*, 1713–1723, 1992.

Bertram, A. K., A. V. Ivanov, M. Hunter, L. T. Molina, and M. J. Molina, The reaction probability of OH on organic surfaces of tropospheric interest, *J. Phys. Chem. A*, *105*, 9415–9421, 2001.

Bertschi, I., R. J. Yokelson, D. E. Ward, R. E. Babbitt, R. A. Susott, J. G. Goode, and W. M. Hao, Trace gas and particle emissions from fires in large diameter and belowground biomass fuels, *J. Geophys. Res.*, *108*(D13), 8472, doi:10.1029/2002JD002100, 2003a.

Bertschi, I. T., R. J. Yokelson, D. E. Ward, T. J. Christian, and W. M. Hao, Trace gas emissions from the production and use of domestic biofuels in Zambia measured by open-path Fourier transform infrared spectroscopy, *J. Geophys. Res.*, *108*(D13), 8469, doi:10.1029/2002JD002158, 2003b.

Christian, T. J., B. Kleiss, R. J. Yokelson, R. Holzinger, P. J. Crutzen, J. Williams, W. M. Hao, and T. Shirai, Comprehensive laboratory measurements of biomass-burning emissions: 2. First intercomparison of open-path FTIR, PTR-MS, GC-MS/FID/ECD, *J. Geophys. Res.*, *108*, doi:10.1029/2003JD003874, in press, 2003a.

Christian, T. J., B. Kleiss, R. J. Yokelson, R. Holzinger, P. J. Crutzen, D. E. Ward, B. H. Saharjo, and W. M. Hao, Comprehensive laboratory measurements of biomass-burning emissions: 1. The emissions from Indonesian, African, and other fuels, *J. Geophys. Res.*, *108*, doi:10.1029/2003JD003704, in press, 2003b.

Crutzen, P. J., and M. O. Andreae, Biomass burning in the tropics: Impact on atmospheric chemistry and biogeochemical cycles, *Science*, *250*, 1669–1678, 1990.

Environmental Protection Agency, *Quality Assurance Handbook for Air Pollution Measurement Systems*, vol. III, *Stationary Source Specific Methods*, *Rep. EPA-600/4-77-027b*, sect. 3.11, Jan. 1982.

Goode, J. G., R. J. Yokelson, R. A. Susott, and D. E. Ward, Trace gas emissions from laboratory biomass fires measured by Fourier transform infrared spectroscopy: Fires in grass and surface fuels, *J. Geophys. Res.*, *104*, 21,237–21,245, 1999.

Goode, J. G., R. J. Yokelson, D. E. Ward, R. A. Susott, R. E. Babbitt, M. A. Davies, and W. M. Hao, Measurements of excess O_3, CO_2, CO, CH_4, C_2H_4, C_2H_2, HCN, NO, NH_3, HCOOH, CH_3OOH, HCHO, and CH_3OH, in 1997 Alaskan biomass burning plumes by airborne Fourier transform infrared spectroscopy (AFTIR), *J. Geophys. Res.*, *105*, 22,147–22,166, 2000.

Griffith, D. W. T., W. G. Mankin, M. T. Coffey, D. E. Ward, and A. Riebau, FTIR remote sensing of biomass burning emissions of CO2, CO, CH4, CH2O, NO, NO2, NH3 and N2O, in *Global Biomass Burning: Atmospheric, Climatic, and Biospheric Implications*, edited by J. S. Levine, pp. 230–239, MIT Press, Cambridge, Mass., 1991.

Holzinger, R., C. Warneke, A. Hansel, A. Jordan, W. Lindinger, D. H. Scharffe, G. Schade, and P. J. Crutzen, Biomass burning as a source of formaldehyde, acetaldehyde, methanol, acetone, acetonitrile, and hydrogen cyanide, *Geophys. Res. Lett.*, *26*, 1161–1164, 1999.

Langmuir, I., The adsorption of gases on plane surfaces of glass, mica, and platinum, *J. Am. Chem. Soc.*, *40*, 1361–1375, 1918.

Lee, J. H., Y. Chen, and I. N. Tang, Heterogeneous loss of gaseous H_2O_2 in an atmospheric air sampling system, *Environ. Sci. Technol.*, *25*, 339–342, 1991.

Mason, S. A., R. J. Field, R. J. Yokelson, M. A. Kochivar, M. R. Tinsley, D. E. Ward, and W. M. Hao, Complex effects arising in smoke plume simulations due to inclusion of direct emissions of oxygenated organic species from biomass combustion, *J. Geophys. Res.*, *106*, 12,527–12,539, 2001.

Neuman, J. A., L. G. Huey, T. B. Ryerson, and D. W. Fahey, Study of inlet materials for sampling atmospheric nitric acid, *Environ. Sci. Technol.*, *33*, 1133–1136, 1999.

Owens, M. A., C. C. Davis, and R. R. Dickerson, A photothermal interferometer for gas-phase ammonia detection, *Anal. Chem.*, *71*, 1391–1399, 1999.

Roscoe, H. K., and K. C. Clemitshaw, Measurement techniques in gas-phase tropospheric chemistry: A selective view of the past, present, and future, *Science*, *276*, 1065–1072, 1997.

Sauren, H., B. van Hove, W. Tonk, H. Jalink, and D. Bicanic, On the adsorption properties of ammonia to various surfaces, in *Monitoring of Gaseous Pollutants With Tunable Diode Lasers*, edited by R. Grisar et al., pp. 196–201, Kluwer Acad., New York, 1989.

Schiff, H. I., D. R. Karecki, G. W. Harris, D. R. Hastie, and G. I. Mackay, A tunable diode laser system for aircraft measurements of trace gases, *J. Geophys. Res.*, *95*, 10,147–10,153, 1990.

Singh, H. B., M. Kanakidou, P. J. Crutzen, and D. J. Jacob, High concentrations and photochemical fate of oxygenated hydrocarbons in the global troposphere, *Nature*, *378*, 50–54, 1995.

van Hove, L. W. A., E. H. Adema, W. J. Vredenberg, and G. A. Pieters, A study of the adsorption of NH_3 and SO_2 on leaf surfaces, *Atmos. Environ.*, *23*, 1479–1486, 1989.

Webster, C. R., R. D. May, C. A. Trimble, R. G. Chave, and J. Kendall, Aircraft (ER-2) laser infrared absorption spectrometer (ALIAS) for in situ stratospheric measurements of HCl, N_2O, CH_4, NO_2, and HNO_3, *Appl. Opt.*, *33*, 454–472, 1994.

Wert, B. P., A. Fried, B. Henry, and S. Cartier, Evaluation of inlets used for the airborne measurement of formaldehyde, *J. Geophys. Res.*, *107*(D13), 4163, doi:10.1029/2001JD001072, 2002.

White, J. U., Long optical paths of large aperture, *J. Opt. Soc. Am.*, *32*, 285–288, 1942.

Worden, H., R. Beer, and C. P. Rinsland, Airborne infrared spectroscopy of 1994 western wildfires, *J. Geophys. Res.*, *102*, 1287–1299, 1997.

Yokelson, R. J. and I. T. Bertschi, Vibrational spectroscopy in the study of fires, in *Handbook of Vibrational Spectroscopy*, vol. 4, edited by J. M. Chalmers and P. R. Griffiths, pp. 2879–2886, John Wiley, Hoboken, N. J., 2002.

Yokelson, R. J., D. W. T. Griffith, and D. E. Ward, Open-path Fourier transform infrared studies of large-scale laboratory biomass fires, *J. Geophys Res.*, *101*, 21,067–21,080, 1996.

Yokelson, R. J., R. Susott, D. E. Ward, J. Reardon, and D. W. T. Griffith, Emissions from smoldering combustion of biomass measured by open-path Fourier transform infrared spectroscopy, *J. Geophys. Res.*, *102*, 18,865–18,877, 1997.

Yokelson, R. J., J. G. Goode, D. E. Ward, R. A. Susott, R. E. Babbitt, D. D. Wade, I. T. Bertschi, D. W. T. Griffith, and W. M. Hao, Emissions of formaldehyde, acetic acid, methanol, and other trace gases from biomass fires in North Carolina measured by airborne Fourier transform infrared spectroscopy, *J. Geophys. Res.*, *104*, 30,109–30,125, 1999.

Yokelson, R. J., I. T. Bertschi, T. J. Christian, P. V. Hobbs, D. E. Ward, and W. M. Hao, Trace gas measurements in nascent, aged, and cloud-processed smoke from African savanna fires by airborne Fourier transform infrared spectroscopy (AFTIR), *J. Geophys. Res.*, *108*(D13), 8478, doi:10.1029/2002JD002322, 2003.

I. T. Bertschi, Interdisciplinary Arts and Sciences, University of Washington, Bothell, 22011 26th Avenue SE, Bothell, WA 98021, USA. (isaacpb@u.washington.edu)

T. J. Christian and R. J. Yokelson (corresponding author), Department of Chemistry, University of Montana, Missoula, MT 59812, USA. (ted.christian@umontana.edu; byok@selway.umt.edu)

W. M. Hao, USDA Forest Service, Fire Sciences Laboratory, PO Box 8089, Missoula, MT 59807, USA. (whao@fs.fed.us)